http://ansinet.com/itj

ITJ

ISSN 1812-5638

INFORMATION TECHNOLOGY JOURNAL

ANSInet
Asian Network for Scientific Information
308 Lasani Town, Sargodha Road, Faisalabad - Pakistan

Information Technology Journal 11 (7): 859-867, 2012
ISSN 1812-5638 / DOI: 10.3923/itj.2012.859.867

Structural Parameter Optimization for 3-DOF Spherical Parallel Mechanism, Binocular Stereo

[1]Shaorong Xie, [1,2]Shuping Li, [1,2]Junjie Huang, [1]Hengyu Li and [1]Jun Luo
[1]School of Mechatronics Engineering and Automation,
Shanghai University, Shanghai, 200072, China
[2]School of Mechanical and Power Engineering, HeNan Polytechnic University,
Jiaozuo, 454000, China

Abstract: The movement scope of the human eye is proposed to be the target working space of the bionic eye by analyzing the error of 3 rotational degrees of freedom (3-DOF) Spherical Parallel Mechanism (SPM). The indexes of the worst dexterity and dynamic performance for bionic eye are defined by using the maximum condition number of Jacobian matrix. Reasonable structural parameters are chosen through analysis and comparison in the case of satisfying the special requirements of the bionic eye structure and making the worst dexterity and dynamic performance of target working space better. The experimental results show that the binocular stereo with the optimized parameters is good coincide with the design.

Key words: Spherical parallel mechanism, binocular stereo, dexterity, dynamic performance, Jacobian matrix

INTRODUCTION

Binocular stereo (robot eyes) can be carried on all kinds of mobile robots, underwater robots and flying robots (Zhixiang *et al*., 2011) because of the following advantages: small size, light weight and compact volume, etc. And it can be used in various environments that are dangerous or unsuitable for human such as traffic, military, counter- terrorism, reconnaissance, disaster relief and so on. But bionic eye is often affected by unstructured and bumpy environments, for example, uneven ground for mobile robots (Mehrjerdi *et al*., 2010), surge for underwater robots, wind speed for flying robots, etc. Those not only cause instability or distortion of the receiving images but also increase the difficulties of observing images by human eyes and processing images by computers (Maohai *et al*., 2011; Quan and Ming, 2011). So far, many bionic eyes have been designed. But in many cases, these designed bionic eyes only achieve one-dimensional or two-dimensional rotation and lack of torsion (Itoh *et al*., 2006; Maini *et al*., 2008; Batista *et al*., 2000; Yu and Wang, 2004). One or two axes of bionic eyes could provide images that can be digitalized and vision processed to compensate for distortions. However, the torsion axes are crucial for realizing accurate human eye captured images with a proper sampling rate. Besides, the software compensation process for a missing torsional rotation is computationally complex and simultaneously disables data acquisition. Only with the third torsion axis can the received images be realized in 3D properly. But little attention has been paid to emulate the actual mechanics of the eye (Bang *et al*., 2006).

Spherical Parallel Mechanism (SPM) has 3 rotational degrees of freedom (3-DOF) which can offer excellent dynamic performance, light weight, high speed and high precision (Gosselin and St-Pierre, 1997). Those just coincide with the characteristics of bionic eye requirements. So it is appropriate that SPM is applied in bionic eye design. The method of global dimensional synthesis was often applied for previous design of spherical parallel mechanism which optimized the global performance indexes and got orthogonal spherical parallel mechanism (Gosselin and St-Pierre, 1997; Liu, 1999; Jin and Rong, 2007). However, bionic eye has special space and structure requirements which is different from those fields. If bionic eye is designed with orthogonal spherical parallel mechanism, it would result in being a larger prototype, no meeting the working space requirements and interfering easily between components.

System description: As shown in Fig. 1, the SPM is composed of a moving platform (end-effector) and a fixed base that are connected by three equally spaced limbs, each consisting of revolute joints only. The axes of all joints intersect at a common point O which is named the SPM center. The motion of any point in the mechanism

Corresponding Author: Shuping Li, M8-208 Room, 149 Yanchang Road, Zhabei District, Shanghai, 200072, China
Tel: +86-21-56334842 Fax: +86-21-56334842

$\beta_1 = 25° \beta_2 = 125° \beta_1 = 25° \beta_2 = 130° \beta_1 = 25° \beta_2 = 135°$

$\beta_1 = 30° \beta_2 = 125° \beta_1 = 30° \beta_2 = 130° \beta_1 = 30° \beta_2 = 135°$

$\beta_1 = 30° \beta_2 = 125° \beta_1 = 35° \beta_2 = 130° \beta_1 = 35° \beta_2 = 135°$

$\beta_1 = 30° \beta_2 = 125° \beta_1 = 35° \beta_2 = 130°$

$\beta_1 = 25° \beta_2 = 125° \beta_1 = 35° \beta_2 = 130°$

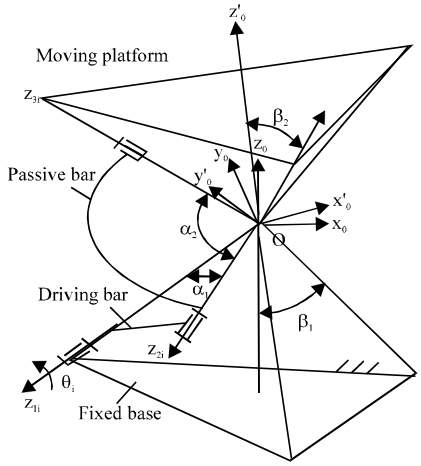

Fig. 1: The structures of SPM

rotates about the point O thereby a spherical parallel manipulator provides three degrees of freedom of pure rotations. According to the method of D-H (Zhangqi *et al*., 2011) linkage coordinate system, a fixed coordinate system O-x_0 y_0 z_0, moving coordinate system O-x_0' y_0' z_0' and linkage coordinate system O-x_{ij} y_{ij} z_{ij} (i, j =1, 2, 3,..., i, j, denotes the jth revolute joint of ith limb) are set up. The plane paralleling to the fixed platform and passing the SPM center is called middle plane (Fig. 2). Since, the manipulator should be symmetric, the structural parameters of a 3-DOF SPM can be reduced to four geometrical angles α_1, α_2, β_1 and β_2, which is shown in Fig. 1. α_1, α_2 are, respectively defined as the angle between axis z_{1i} and z_{2i}, axis z_{3i} and z_{3i}, β_1, β_2, respectively means semi-cone angle of the fixed base, semi-cone angle of the moving platform. u_i, w_i, v_i (i = 1, 2, 3) denotes unit vector of coordinate-axis z_{1i}, z_{2i}, z_{3i} (i = 1, 2, 3) for fixed coordinate system, respectively.

Moving platform (the eye) attitude can be expressed by direction cosine matrix R_{XYZ} of moving coordinate system O-x_0' y_0' z_0' to fixed coordinate system O-x_0 y_0 z_0 (Gosselin and St-Pierre, 1997):

$$R_{XYZ} = \begin{bmatrix} c\phi_y c\phi_z & s\phi_x s\phi_y c\phi_z - c\phi_x s\phi_z & c\phi_x s\phi_y c\phi_z + s\phi_x s\phi_z \\ c\phi_y s\phi_z & s\phi_x s\phi_y s\phi_z + c\phi_x c\phi_z & c\phi_x s\phi_y s\phi_z - c\phi_x c\phi_z \\ -s\phi_y & s\phi_x c\phi_y & c\phi_x c\phi_z \end{bmatrix} \quad (1)$$

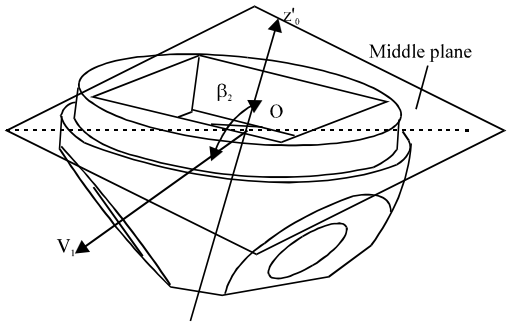

Fig. 2: The moving platform and β_2

where, ϕ_x, ϕ_y, ϕ_z denotes yaw, pitch, roll angles of bionic eye, respectively. S• and C• represents sin and cos, respectively.

The inverse kinematics solution: The inverse kinematics is that three input angles of motor (θ_1, θ_2, θ_3) are solved through the known three attitude angles of bionic eye (ϕ_x, ϕ_y, ϕ_z) (Zhangqi *et al*., 2011). Closed loop equation can be obtained from Alternate angle Law (Cong *et al*., 2011):

$$w_i \bullet v_i = \cos \alpha_2 \; i = 1, 2, 3 \quad (2)$$

Direction vector of u_i, w_i, v_i in fixed coordinate system O-x_0 y_0 z_0 can be obtained by attitude transformation. The inverse kinematics solution can be figured out from formula 2 (Gosselin and St-Pierre, 1997).

Jacobian matrix: The Eq. 3 is established by differentiation of formula 2 and utilizing the mixed product of vectors:

$$\dot{\theta}_{1i}(u_i \times w_i) \bullet v_i = \omega \bullet (w_i \times v_i) \; i = 1,2,3 \quad (3)$$

As also showed in matrix form:

$$\dot{\theta} = J_2^{-1} J_1 \omega = J\omega \quad (4)$$

where, $\dot{\theta} = (\dot{\theta}_1, \dot{\theta}_2, \dot{\theta}_3)^T$ represents angular velocity vector of motor, $\omega = (\omega_x, \omega_y, \omega_z)^T$ represents angular velocity vector of moving platform, $J_1 = \text{diag}\,[b_1, b_2, b_3]$, $b_i = (u_i \times w_i)^T \bullet v_i$ represents the first kind of Jacobian matrix, $J_2 = [w_1 \times v_1, w_2 \times v_2, w_3 \times v_3]^T$ represents the second kind of Jacobian matrix. J denotes Jacobian matrix which is determined by four structural parameters α_1, α_2, β_1, β_2 and three attitude angles ϕ_x, ϕ_y, ϕ_z.

The dexterity performance index: Salisbury and Craig (1981) defined the dexterity of a robotic manipulator as the kinematic accuracy. Mathematically, they defined the dexterity as the condition number of the Jacobian matrix of the robot. The dexterity of the 3-DOF SPM, noted k, can then be written as follow (Gosselin and St-Pierre, 1997):

$$k(J) = \|J\| \|J^{-1}\| \quad (5)$$

where, ||J|| denotes any norm of its matrix.

It is bounded as follows:

$$1 \le k(J) \le \infty \quad (6)$$

And hence, the reciprocal of the condition number (noted and referred to here as the dexterity of the manipulator) is used instead.

$$\zeta = \frac{1}{k(J)} = \frac{1}{\|J\|\|J^{-1}\|} \quad (7)$$

where, $0 \le \zeta \le 1$, ζ vary with the configuration of the robot and the structural parameters of the robot. A value of ζ equal or close to 1 corresponds to a configuration with a very good kinematic accuracy while a value of ζ equal to 0 is obtained when the manipulator is in a singular configuration. The bigger the value of ζ is, the better the dexterity and control accuracy of the robot are.

Dynamic performance index: Dynamic performance index can be expressed as below (Liu, 1999):

$$0 < \xi = \frac{1}{k(G)} = \frac{1}{\|G\|\|G^{-1}\|} \le 1 \quad (8)$$

where, ξ denotes dynamic performance index of the robot. The bigger the value of ξ is, the better the dynamic performance of the robot is.

The target working space and preliminary optimization of structural parameters

The target working space: The eye-ball is assumed to be modeled as a homogeneous sphere of radius R, having 3 rotational degrees of freedom about its center and the largest range of human eyes can be pointed in a vision cone of ±38° with ±15° in torsion (Cannata and Maggiali, 2006). There exist errors where in the process of SPM movement, key parts processing and assembling, revolute joints clearance, servo control, position drift for angular pyramid vertex of moving platform relative to fixed base, component thermo-elastic distortion (Zeng *et al*., 2008; Ab-Rahman *et al*., 2011; Suhail *et al*., 2011) which would make the actual working space is slightly bigger than the target working space. Therefore, the target working space for the prototype is designed a cone of ±38° with ±15° in torsion (in a cone of 38°, any position can achieve at least 15° in torsion). The maximum semi-cone angle approximately reached 40° that was shown in the final experimental results.

Preliminary optimization of structural parameters: According to the special structure requirements of bionic eye, relative parameters are preliminarily optimized before optimizing the structural parameters.

α_1 and α_2 (structure angles of driving bar and passive bar): theoretically, the range of α_1 and α_2 are both (0, 180°). Excessive small value of α_1 and α_2 would cause the working space too small and does not meet the design requirements but also bring difficulty to assemble the bionic eye. Excessive large value of α_1 and α_2 would result in a larger prototype of bionic eye, interfering easily between components, besides, it may make the passive bar locate above middle plane in the movement course which leads to block the camera view and interfere with robot's face. Thus, the range of α_1 and α_2 are set as: (50°, 80°).

β_1 (semi-cone angle of the fixed base): The center of the revolute joints of each limb locating on the different radius of the sphere rotating the point O, In order that the limbs can't be interfered with each other. The different radius of sphere mentioned above are denoted as $R_{Z_{1i}}, R_{Z_{2i}}, R_{Z_{3i}}$, respectively and moreover, $R_{Z_{1i}} > R_{Z_{2i}} > R_{Z_{3i}}$. This does not affect the dexterity. In this case, the greatest impact on overall size of bionic eye is the radius of fixed base ($R_{base} = R_{Z_{1i}} \sin\beta_1$). In the case of $R_{Z_{1i}}$ being constant, the greatest impact on overall size of bionic eye is the angle of β_1, with the decreasing of the angle of β_1, R_{base} will decrease exponentially. In addition, in order to avoid the interference with the three motors when β_1 is too small, the range of β_1 is set as: (25°, 35°).

β_2 (semi-cone angle of the moving platform): Many papers (Cong *et al*., 2011; Liu, 1999; Jin and Rong, 2007) have put forward the range of β_2 are (0, 90°). But this is not appropriate for the design of bionic eye. On one hand, it is ensure that the imaging focus of built-in camera is just located in the point O, so that the deflection of bionic eye is consistent with that of the eyeball. On the other hand, it is also ensure that the driving bars and the passive bars located below the middle plane in the movement course which do not block the camera view and do not interfere with the robot's face. Based on above considerations, the value of β_2 must be more than 90°, i.e., the moving platform must locate blow the middle plane (Fig. 2).

Besides, it is considered that the three passive bars connecting with the bionic eye can not interfere with each other. The range of β_2 is set as: (125°, 135°).

STRUCTURAL PARAMETERS OPTIMIZATION DESIGN

The minimum values of dexterity and dynamic performance indexes in target working space: The method of global dimensional synthesis takes the average performance index of workspace as the optimizing object. With this method, the design parameters are determined and the average performance index is very good but it does not make arbitrary posture dexterity of target working space better. However, the method optimized the minimum performance index can make the dexterity and dynamic performance of bionic eye all over the target workspace better.

Put force Jacobian matrix $G = (J^{-1})^T$ (Liu, 1999) into formula 9, we can obtain:

$$0 < \xi = \frac{1}{k(G)} = \frac{1}{\|G\|\|G^{-1}\|} = \frac{1}{\|(J^{-1})^T\|\|J^T\|} \le 1 \quad (9)$$

Similarly, dynamic performance can be expressed as below:

$$k(g) = \|G\|\|G^{-1}\| = \|(J^{-1})^T\|\ \|J^T\| \quad (10)$$

According to formula 10, properties of matrix and norm, we can obtain:

$$\|J\|_2\|J^{-1}\|_2 = \|(J^{-1})^T\|_2\|J^T\|_2 = \|G\|_2\|G^{-1}\|_2,$$
$$\|J\|_F\|J^{-1}\|_F = \|(J^{-1})^T\|_F\|J^T\|_F = \|G\|_F\|G^{-1}\|_F,$$
$$\|J\|_\infty\|J^{-1}\|_\infty = \|(J^{-1})^T\|_1\|J^T\|_1 = \|G\|_1\|G^{-1}\|_1,$$
$$\|J\|_1\|J^{-1}\|_1 = \|(J^{-1})^T\|_\infty\|J^T\|_\infty = \|G\|_\infty\|G^{-1}\|_\infty$$

($\|\bullet\|_1$, $\|\bullet\|_2$, $\|\bullet\|_F$, $\|\bullet\|_\infty$ denote 1-norm, 2-norm, F-norm, infinity-norm, respectively). That is to say, the values of k(J) and k(G) under 2-norm and F-norm are equal, respectively. The values of k(J) under infinity-norm and the values of k(G)under 1-norm are equal, respectively. The values of k(J) under 1-norm and the values of k(G) under infinity-norm are equal, respectively.

In order to obtain the minimum values of ζ and ξ from Eq. 7 and 8, the maximum values of velocity Jacobian matrix condition number k(J) from Eq. 5 and force Jacobian matrix condition number k(G) from Eq. 10 should be obtained. In the case that target working space is determined, ranges of four parameters are optimized preliminarily and each element absolute value in velocity and force Jacobian matrix is mostly between 0 and 1. The values of k(J) and k(G) under 1-norm, 2-norm, F-norm and infinity-norm are compared and lots of experimental data is shown that the maximum values of k(J) and k(G) always arise under 1-norm and infinity-norm. Parts of data are only listed in Table 1.

So, we defined the minimum values of dexterity and dynamic performance indexes in target working space as:

$$\xi_{min} = \min\left(\frac{1}{\|J\|\|J^{-1}\|}\right) = \frac{1}{\|J\|_\infty\|J^{-1}\|_\infty} = \frac{1}{\|G\|_1\|G^{-1}\|_1} \quad (11)$$

$$\xi_{min} = \min\left(\frac{1}{\|G\|\|G^{-1}\|}\right) = \frac{1}{\|G\|_\infty\|G^{-1}\|_\infty} = \frac{1}{\|J\|_1\|J^{-1}\|_1} \quad (12)$$

Dexterity and dynamic performance are all considered under 1-norm and infinity-norm in formula 11 and 12 which ensures that the values of dexterity and dynamic performance indexes are the minimum.

Structural parameter optimization with step method: The purpose of this design is to determine four design parameters α_1, α_2, β_1, β_2 and make values ζ_{min} and ξ_{min} to be maximum by satisfying the special structure requirements and the target working space of the bionic eye.

Parameters optimization program is developed in MATLAB. The best structural parameters are searched with step method. Based on the known values of β_1 and β_2, we change the values of α_1 and α_2 from small to large number with 1° for step. Finally, the maximum values of ζ_{min} and ξ_{min} are obtained.

Figure 3 is the relationship between ζ_{min} and α_1, α_2, β_1, β_2 with different values of β_1 and β_2, Fig. 4 is the

Table 1: Values of k(J) and k(G) under four norm with different values of α_1, α_2, β_1, β_2

Different values of α_1, α_2, β_1, β_2	Values of k(J) under 1-norm (values of k(G) under infinity-norm)	Values of k(J) under 2-norm (values of k(G) under 2-norm)	Values of k(J) under F-norm (values of k(G) under F-norm)	Values of k(J) under infinity-norm (values of k(G) under 1-norm)
$\alpha_1 = 50°$, $\alpha_2 = 50°$, $\beta_1 = 25°$, $\beta_2 = 125°$	193.6562	136.4782	163.2379	232.1222
$\alpha_1 = 50°$, $\alpha_2 = 50°$, $\beta_1 = 25°$, $\beta_2 = 130°$	190.4309	134.4378	156.2966	217.8983
$\alpha_1 = 50°$, $\alpha_2 = 50°$, $\beta_1 = 35°$, $\beta_2 = 135°$	9.6443	6.0115	7.3105	7.4326
$\alpha_1 = 75°$, $\alpha_2 = 75°$, $\beta_1 = 25°$, $\beta_2 = 125°$	5.6616	3.0318	4.4723	4.4343
$\alpha_1 = 75°$, $\alpha_2 = 75°$, $\beta_1 = 30°$, $\beta_2 = 130°$	7.0441	5.5499	6.7320	7.5504
$\alpha_1 = 75°$, $\alpha_2 = 75°$, $\beta_1 = 35°$, $\beta_2 = 135°$	55.8939	41.3370	45.6729	58.2878
$\alpha_1 = 80°$, $\alpha_2 = 80°$, $\beta_1 = 25°$, $\beta_2 = 125°$	5.7032	2.6935	4.3156	4.6107
$\alpha_1 = 80°$, $\alpha_2 = 80°$, $\beta_1 = 30°$, $\beta_2 = 130°$	6.5546	5.0972	6.3110	8.0468
$\alpha_1 = 80°$, $\alpha_2 = 80°$, $\beta_1 = 35°$, $\beta_2 = 135°$	76.8163	61.7406	68.0186	83.1632

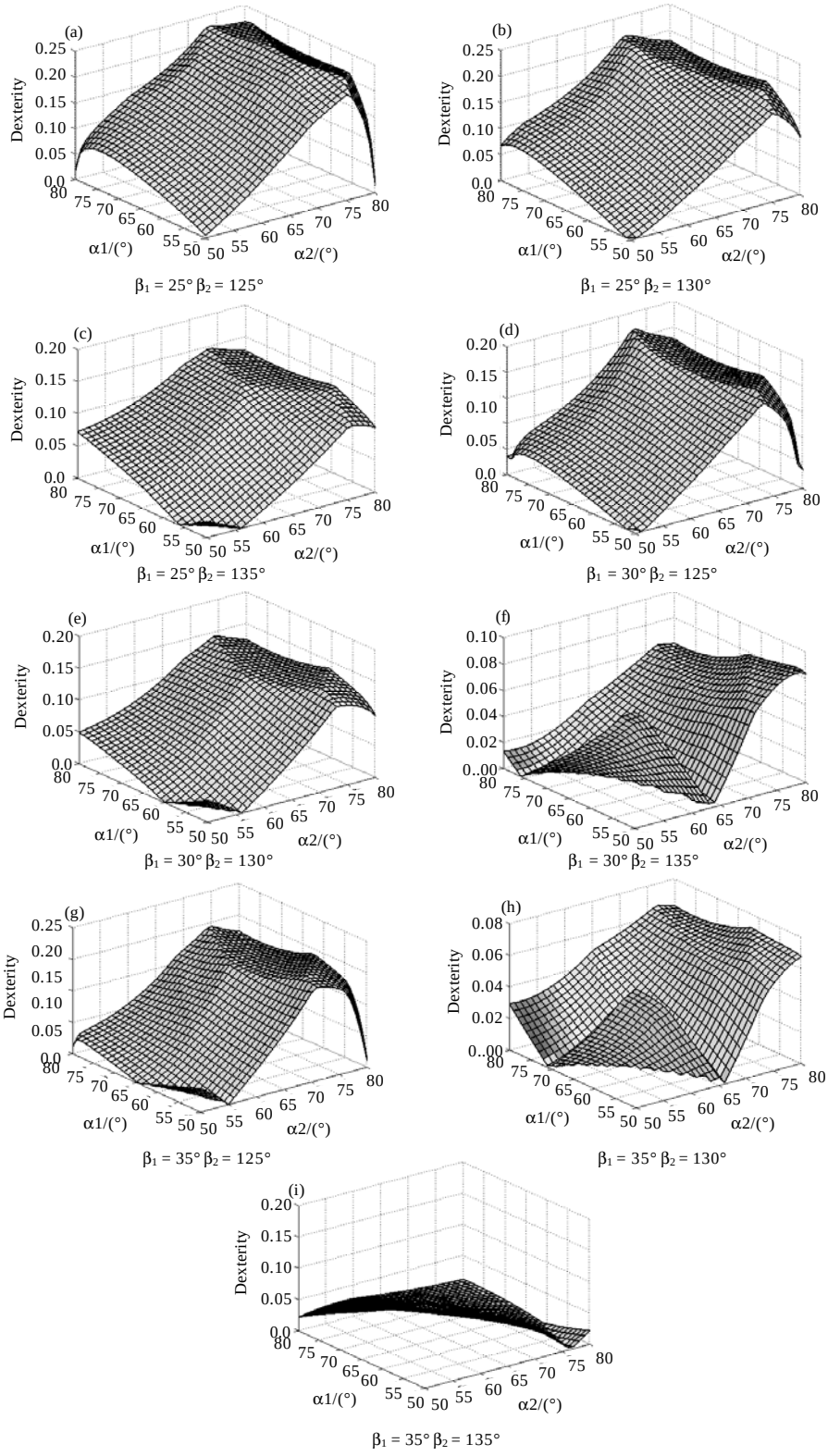

Fig. 3(a-i): The relationship between ζ_{min} and α_1, α_2, β_1, β_2

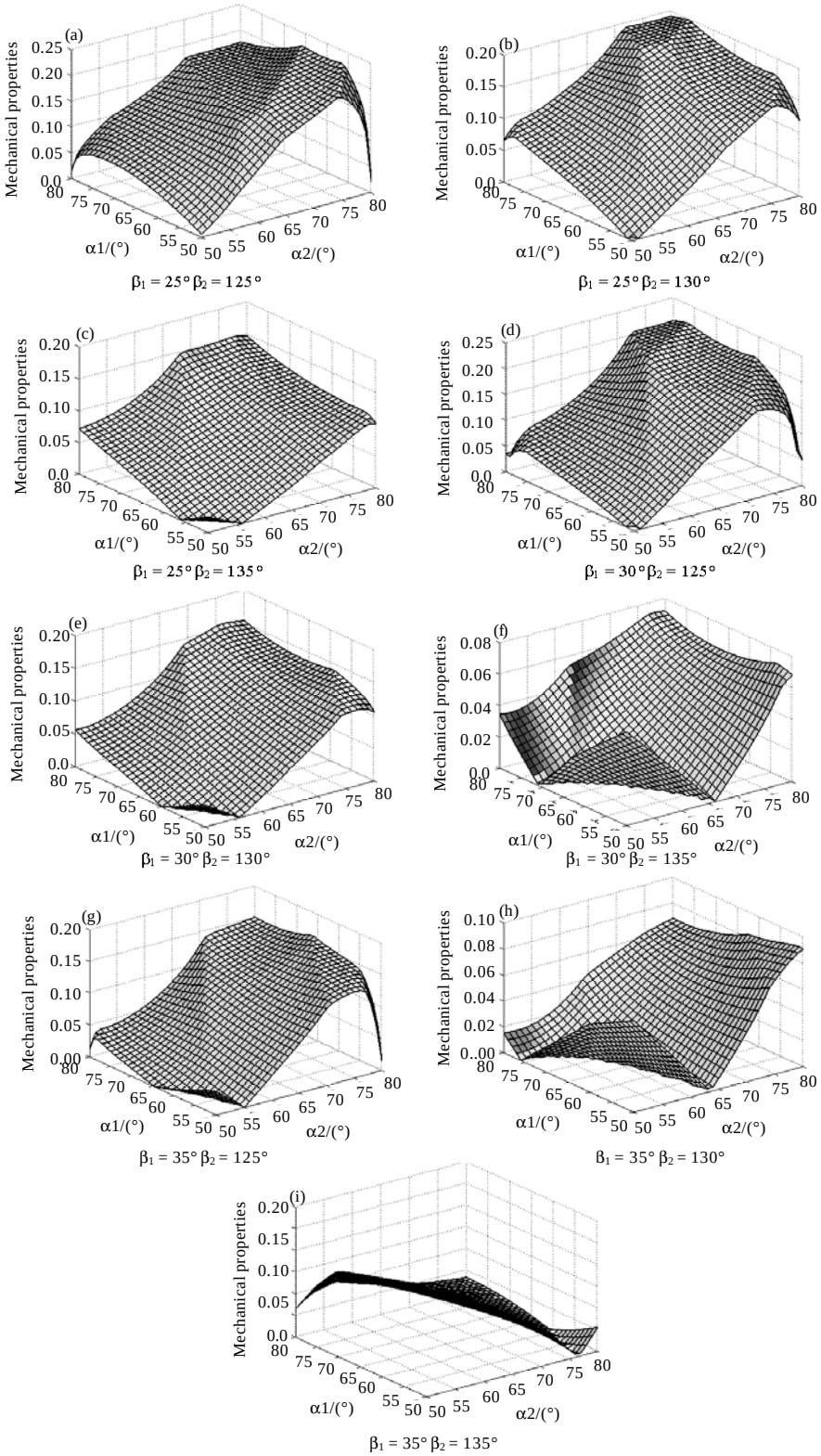

Fig. 4(a-i): The relationship between ξ_{min} and $\alpha_1, \alpha_2, \beta_1, \beta_2$

Fig. 5(a-c): Experimental platform based on tracked robot

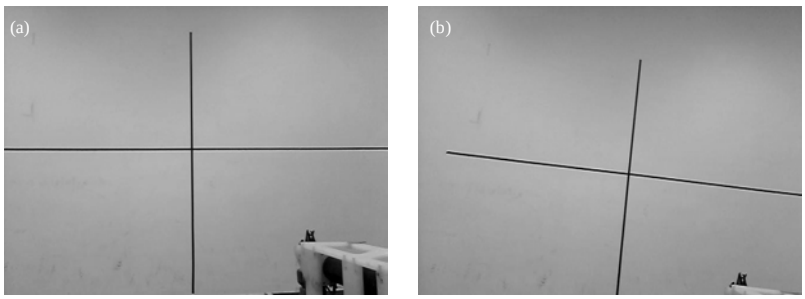

Fig. 6(a-b): Experimental results under harsh environment

relationship between ξ_{min} and α_1, α_2, β_1, β_2 with different values of β_1 and β_2 From Fig. 3 and 4, it is known that when $25° \le \beta_1 \le 35°$ and $125° \le \beta_2 \le 135°$, the maximum values of ζ_{min} and ξ_{min} are mostly located in $\alpha_1 = 75°$, 80° and $\alpha_2 = 75°$ nearby. Meanwhile, ζ_{min} and ξ_{min} decrease along with the increase of β_1 and β_2. According to the analysis, it was found that when $\beta_1 = 25°$ β_2 125°, $\beta_1 = 25°$ β_2 130° and $\beta_1 = 30°$ β_2 125°, the maximum values of ζ_{min} are all better. When $\beta_1 = 30°$ β_2 125°, the maximum values of ζ_{min} are best. Finally, considering dexterity and dynamic performance indexes, we select $\alpha_1 = 75°$, $\alpha_2 = 75°$, $\beta_1 = 30°$, $\beta_2 = 125°$.

ROBOT EXPERIMENT

Some experiments based on a tracked robot equipping with bionic eye are implemented in a bumpy environment. The experimental platform is developed, as shown in Fig. 5. A robot control and image processing module is shown in Fig. 5a. The tracked robot carrying binocular stereo is presented in Fig. 5b. An enlargement of bionic eye with SPM is demonstrated in the Fig. 5c.

One can obviously find two interesting results in the experiment. First, binocular stereo have good dexterity and dynamics performance, operating flexibility, no mutual interference in the target working space for any posture. In the actual operation process, we found that the actual workspace of the bionic eye is slightly bigger than the target working space and semi-cone angle can approximately reach 40°. Second, binocular stereo have very good adaptive ability and it can actively compensate the visual error caused by robot attitude variation. Stabilization image can be obtained even under bumping environment.

Parts of the experimental results are shown in Fig. 6. Figure 6 a and b are the experimental results when the tracked robot attitude occurs roll (a, compensating for the attitude; b, without compensation for the attitude.

CONCLUSION

In this study, a 3-DOF spherical parallel manipulator is presented and the prototype of the 3-RRR spherical parallel binocular Stereo has been built in the lab (Fig. 5b). Specifically, the worst dexterity and dynamic performance index for bionic eye is defined by the maximum condition number of Jacobian matrix. The chart method is used to search for optimal design parameters and reasonable structural parameters are chosen in the case of satisfying the special structure requirements of bionic eye. The techniques used in this study can also be applied to he optimization of other parallel manipulators. Finally, the experimental results show that bionic eye with the optimized parameters is good coinciding with the design requirements. The size of bionic eye is slightly bigger than that of the actual eyeball in consideration of camera size (31×31 mm), those radius are 45 and 30 mm, respectively. It was found that the violent vibration of robot body and visual inertial navigation drifts would affect the accuracy of the bionic eye. Those would be taken into account for designing bionic eye in the future.

ACKNOWLEDGMENTS

This project is supported by National Hi-tech Research and Development Program of China (863 Program, Grant No. 2009AA04Z211), National Natural Science Foundation of China (Grant No. 50975168, Grant No. 60975068) and Ph.D. Programs Foundation of Ministry of Education of China (Grant No. 20093108110007).

REFERENCES

Ab-Rahman, M.S., M. Tanra, S.C.R. Boonchuan Ng, A. Baharudin and S.A.M. Khithir, 2011. Analysis of components failure, malfunction effect and prevention technique in customer access network FTTH-PON. J. Applied Sci., 11: 201-211.

Bang, Y.B., J.K. Paik, B.H. Shin and C. Lee, 2006. A three-degree-of-freedom anthropomorphic oculomotor simulator. Inter. J. Control, Automa. Syst., 4: 227-235.

Batista, J., P. Peixoto and H. Araujo, 2000. Binocular tracking and accommodation controlled by retinal motion flow. Proc. Inter. Conf. Pattern Recognit., 1: 171-174.

Cannata, G. and M. Maggiali, 2006. Implementation of listing's law for a robot eye. Proceedings of the International Conference on Intelligent Robots and Systems, October 9-15, 2006, Beijing, China, pp: 3940-3945.

Cong, M., Y. Wu, D. Liu, Y. Du, H. Wen and J. Yu, 2011. Simulation of 6-DOF parallel robot for coupling compensation method. Inform. Technol. J., 10: 428-433.

Gosselin, C.M. and E. St-Pierre, 1997. Development and experimentation of a fast 3-DOF camera-orienting device. Int. J. Rob. Res., 16: 619-630.

Itoh, K., H. Miwa and M. Zecca, 2006. Mechanical design of emotion expression humanoid robot WE-4RII. Proceedings of 16th Symposium on Theory and Practice of Robots and Manipulators, Jun 21-24, 2006, Warsaw, Poland, pp: 255-262.

Jin, Z. and Y. Rong, 2007. Design of a waist joint based on three branches unequal spaced distribution spherical parallel manipulator. China Mech. Eng., 18: 2697-2699.

Liu, X., 1999. The relationships between the performance criteria and link lengths of the parallel manipulators and their design theory. Ph.D. Thesis, Yan shan University, Qinhuangdao.

Maini, E.S., L. Manfredi, C. Laschi and P. Dario, 2008. Bioinspired velocity control of fast gaze shifts on a robotic anthropomorphic head. J. Auton Robot., 25: 37-58.

Maohai, L., S. Lining, H. Qingcheng, C. Zesu and P. Songhao, 2011. Robust omnidirectional vision based mobile robot hierarchical localization and autonomous navigation. Inform. Technol. J., 10: 29-39.

Mehrjerdi, H., M. Saad, J. Ghommam and A. Zerigui, 2010. Optimized neuro-fuzzy coordination for multiple four wheeled mobile robots. Inform. Technol. J., 9: 1557-1570.

Quan, Z.G. and L.Z. Ming, 2011. Research on preprocessing of color image for vision based mobile robot navigation. Inform. Technol. J., 10: 597-601.

Salisbury, J.K. and J. Craig, 1981. Articulated hands: Force control and kinematic issues. Proceedings of the Joint Automatic Control Conference, June 17-19, 1981, Charlottesville, VA, USA,.

Suhail, A.H., N. Ismail, S.V. Wong and N.A.A. Jalil, 2011. Workpiece surface temperature for in-process surface roughness prediction using response surface methodologyac. J. Applied Sci., 11: 308-315.

Yu, H. and Y. Wang, 2004. Research and development of multi-freedom stereovision navigating system with biological vision mechanisms. J. Hunan Unive., 31: 62-65.

Zeng, X., X. Huang and M. Wang, 2008. Micro-assembly of micro parts using uncalibrated microscopes visual servoing method. Inform. Technol. J., 7: 497-502.

Zhangqi, W., Z. Xiaoguang and H. Qingyao, 2011. Motion modeling and simulation of biped robot. Inform. Technol. J., 10: 2232-2236.

Zhixiang, T., W. Hongtao and F. Chun, 2011. Target capture for free-floating space robot based on binocular stereo vision. Inform. Technol. J., 10: 1222-1227.